

## Flux Droplet Formation in NbSe<sub>2</sub> Single Crystals Observed by Decoration

M. Marchevsky,<sup>1</sup> L. A. Gurevich,<sup>2</sup> P. H. Kes,<sup>1</sup> and J. Aarts<sup>1</sup>

<sup>1</sup>*Kamerlingh Onnes Laboratory, University of Leiden, 2300 RA Leiden, The Netherlands*

<sup>2</sup>*Institute of Solid State Physics, Chernogolovka, Moscow District, 142432, Russia*

(Received 1 May 1995)

A potential barrier of geometrical origin, characterized by a barrier field  $H_p$ , governs vortex penetration in thin superconducting samples. We observed this effect by the decoration of crystals of NbSe<sub>2</sub>. Upon zero field cooling and applying a field  $H_a < H_p \approx 5$  mT, vortices form a belt at the sample edges. At  $H_a \approx H_p$  flux begins to penetrate in the form of dropletlike intrusions. The orientational correlation length for the vortex pattern inside the “droplets” is much larger than for the field-cooled patterns. This we interpret as recrystallization of the moving flux line lattice.

PACS numbers: 74.60.Ge, 74.60.Jg

Penetration of magnetic flux in superconductors recently became again a subject of theoretical and experimental investigations, due to the fact that, in finite samples, “geometrical” effects can significantly affect the critical state and the resulting vortex distribution. This problem was already studied a long time ago, but it was carefully reconsidered recently by Brandt [1], Brandt and Indenbom [2], and Zeldov *et al.* [3,4], who presented calculations of the field and current distributions in thin superconducting strips in perpendicular field. They showed, among other things, some specific consequences of a rectangular sample geometry.

First, in the Meissner state, the screening current persists over the entire width of the superconductive strip. For a sample of width  $2W$  and thickness  $d$ ,  $\lambda \ll d \ll W$ , it is given by [4]

$$J_y(x) = -\frac{2H_a}{d} \frac{x}{\sqrt{W^2 - x^2}} \quad \text{for } |x| < W - \frac{d}{2}, \quad (1)$$

with  $\lambda$  the penetration depth and  $H_a$  the applied field. In the absence of pinning ( $J_c = 0$ ) the cutoff for the edge current should be taken at  $J_e^0 = 2H_{c1}/d$  for  $x \rightarrow W$ , where  $H_{c1}$  is the perpendicular lower critical field. Another consequence of a rectangular cross section is the occurrence of a “geometrical barrier” against flux penetration, as was shown by Indenbom *et al.* [5] and by Zeldov *et al.* [4]. The barrier is characterized by the penetration field  $H_p = H_{c1}\sqrt{d/W}$ . If the applied external field  $H_a$  is less than  $H_p$ , flux lines only enter over a width of about  $d/2$  and form a vortex belt along the sample edges. The shielding current in this case is approximately given by Eq. (1); it flows over the whole width of the sample even in the absence of bulk pinning. For  $H_a > H_p$  vortices are driven towards the sample center by the screening currents. If pinning is low, the geometrical potential governs the flux distribution and Zeldov’s result for  $J_c < J_e^0$  applies. For strong pinning,  $J_c \gg J_e^0$ , field profiles as calculated in Refs. [1,2] are recovered. Clearly, the geometrical effects are best observed in weakly pinning materials.

Below, we show such observations on low pinning NbSe<sub>2</sub>. More interestingly, however, is that we can observe novel dropletlike flux intrusions for  $H_a$  near  $H_p$ .

We used the decoration technique to obtain information about the flux distribution in these samples for different applied fields below and above  $H_p$ . The advantage of the decoration technique is that it allows us to measure the field distribution with single-vortex accuracy and submicron spatial resolution [6,7]. This makes it possible to obtain more detailed information than with other methods, such as magneto-optics [5,8] or the use of miniature Hall probes [4].

Our experiments were performed on 2H-NbSe<sub>2</sub> single crystals. 2H-NbSe<sub>2</sub> is a superconductor with  $T_c = 7.2$  K, London penetration depth  $\lambda_L = 265$  nm, Ginzburg-Landau coherence length  $\xi_{GL}(0) = 7.8$  nm, anisotropy  $\gamma = 3$ , and upper critical field slope near  $T_c$   $dH_{c2}/dT = 0.75$  T/K. NbSe<sub>2</sub> is known to have weak vortex pinning properties and relatively low critical currents, since the layered structure possesses few grain boundaries. The crystals were platelets, with the  $c$  axis normal to the platelet surface. Most of them had a characteristic hexagonal shape, a size of about 1–2 mm and thicknesses in the range of 50–150  $\mu\text{m}$ . From their geometrical dimensions we expected  $H_p$  for our samples to be about 3–5 mT. Samples were cooled down to 1.2 K in low remanent magnetic field (typically 0.1–0.2 mT) and always decorated at this temperature. The external field was applied either at 1.2 or at 4.2 K prior to the decorations at 1.2 K. Experiments were done for three different external fields: 3, 5, and 7.5 mT; more than 10 samples were studied in each case.

The typical flux distribution observed in 3 mT is shown in Fig. 1(a). We see a belt of vortices along the sample edges. Its width varies in a range of 30–50  $\mu\text{m}$ , which is close to the sample half thickness  $d/2 = 65$   $\mu\text{m}$ . Shown in Fig. 1(b) is the field profile  $B_z(x)$  and the corresponding current distribution in the sample as calculated in the strip approximation from the image by using Brandt’s approach [1],

$$J_y(x) = \frac{2}{\pi d} \int_{-W}^W \frac{H_z(u) - H_a}{u - x} \left( \frac{W^2 - u^2}{W^2 - x^2} \right)^{1/2} du \quad \text{for } |x| < W. \quad (2)$$

The obtained dependence is actually very close to the one described by formula (1) for a Meissner current. The edge current  $J_e^0$  at 1.2 K evaluated from  $H_{c1}(1.2 \text{ K}) = 9 \text{ mT}$  is expected to be about  $1 \times 10^4 \text{ A/cm}^2$  for a  $130 \mu\text{m}$  thick sample. This is close to the value of  $J$  calculated with Eq. (2) at the vortex belt interface.

This has to be compared to  $J_c$  in order to see whether the weak pinning scenario applies. Unfortunately,  $J_c$  at these low fields is not very well known. Recent low-field measurements of  $J_c$  performed by Duarte *et al.* [9] give the value  $J_c \approx 5 \times 10^3 \text{ A/cm}^2$ . In our own experiments at 3 and 5 mT we usually observed the field-cooled vortices of the remanent field, 0.1–0.2 mT [see Fig. 1(a)] at close distance to the interface with the belt. This indicates a similar value for  $J_c$ , since apparently the driving force was less than the single-vortex pinning force; otherwise, these vortices would have been driven to the sample center upon applying the external field. The regime we work in is therefore probably  $J_e^0 \gtrsim J_c$ .

Next, we discuss experiments performed at 5 mT external field. Two of many similar images obtained in these experiments are shown in Figs. 2(a) and 2(b). For the sample in Fig. 2(a) (thickness  $80 \mu\text{m}$ , half-width  $\sim 0.5 \text{ mm}$ ) we can estimate  $H_p \approx 4 \text{ mT}$  (at 1.2 K). The actual sample shape and shape imperfections may change this value and make it varying along the edges. Also the sample is heated as a side effect of the decoration experiment. In our case the temperature during decoration went up to 3.9 K, which would decrease  $H_p$  with about 10%. First, we see again the vortex belt, as in the 3 mT experiments. It expands in the middle of each edge and narrows near the corners. Next, we see flux “droplets” that originate from the belt and are elongated towards the sample center. Usually one can observe a few droplets in one sample. Their sizes vary in a wide range from 30 up to 300  $\mu\text{m}$ .

A fascinating feature of the vortex lattice inside the droplets is the very high degree of order, both translational

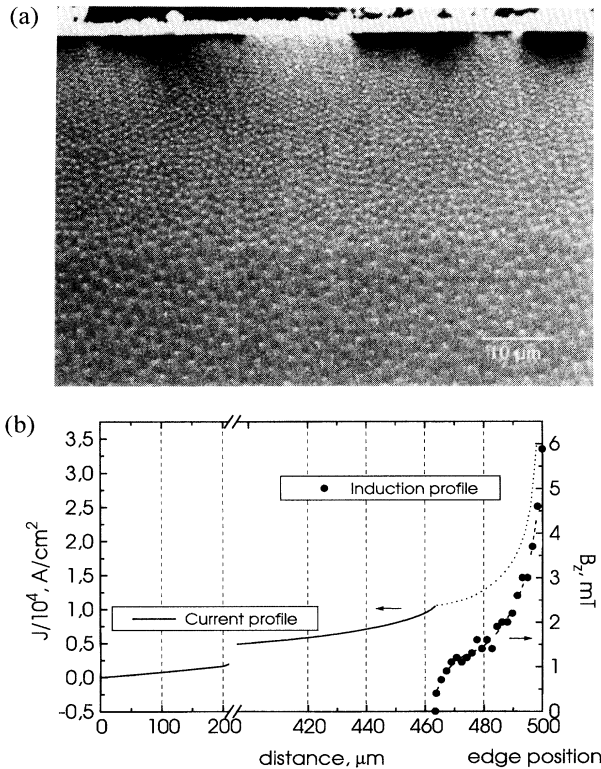


FIG. 1. (a) Decoration pattern of the vortex distribution in the belt near the sample edge,  $H_a = 3 \text{ mT}$ . (b) Induction profile in the sample as measured from the above picture and the corresponding current distribution, calculated (see text) for a sample half-width  $W = 0.5 \text{ mm}$  and thickness  $d = 130 \mu\text{m}$ . The value at the edge was not measured, but fixed at  $H_{\text{edge}} = H_a \sqrt{W/d} \approx 5.9 \text{ mT}$ . Close to the edge the current distribution (dotted) is most affected by the fixed value of  $H_{\text{edge}}$ .

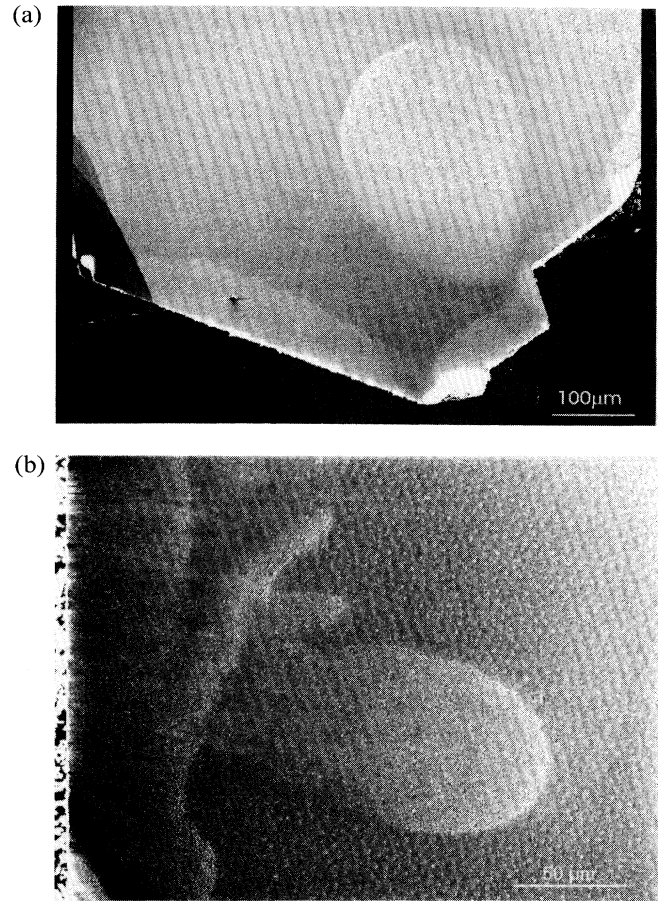


FIG. 2. Decoration patterns obtained on different samples at  $H_a = 5 \text{ mT}$ . Visible are parts of the sample edge, with the belt and droplets originating from it.

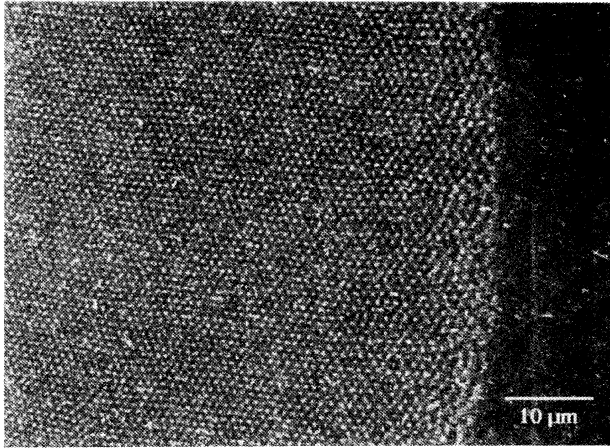


FIG. 3. A higher magnification view of the vortex pattern in the flux droplet close to its front (calculated induction 2.2 mT).

and orientational (see Fig. 3). For the applied field of 5 mT the induction inside the droplets was always substantially lower than the external field, and it was found to be in the range of 1.8–2.5 mT for different samples. Normally droplets consist of a few large grains of an ordered vortex lattice, consisting of up to  $10^4$  vortices. Typically, the average grain size increases when the size of the droplet is larger. The orientational correlation function (OCF) calculated within a grain close to the droplet front is shown in Fig. 4. We can compare this OCF to the results of the field-cooling experiments we did in fields of 0.5, 1.6, and 5 mT. Typically, the correlation length for field-cooled lattices increases with field. We plotted the orientational correlation functions for comparison in the same figure. Fitting them with an exponential decay, we found that the 2.2 mT vortex

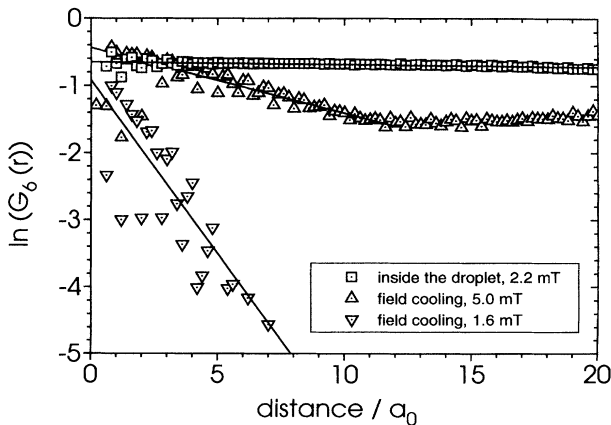


FIG. 4. Orientational correlation functions for a vortex pattern in the droplet (calculated induction 2.2 mT) and for field-cooled lattices at 5 and 1.6 mT. Drawn lines show the exponential fits from which correlation lengths were extracted. The numbers found are  $275a_0$  (droplet, 2400 vortices used in the calculation),  $10.3a_0$  (5 mT FC, 1350 vortices used), and  $1.9a_0$  (1.6 mT FC, 830 vortices used).

pattern inside the droplet has a correlation length that is dramatically (about 20 or 100 times) larger than the correlation length in a field-cooled pattern at 5 and 1.6 mT, respectively.

Therefore we propose the following scenario for the droplet formation process. First, at some point along the edge,  $H_a$  exceeds  $H_p$ . This may be either because the irregular sample shape locally leads to a lower barrier or because the heat pulse of the decoration procedure decreases  $H_p$ . This allows the screening current to drive the vortices in the barrier region towards the center. Now the motion becomes important. According to Ref. [10], a moving vortex configuration will spontaneously recrystallize to a “perfect” vortex crystal, if the driving force acting on the vortices overcomes a certain critical value. For weak pinning materials this critical value is expected to be only slightly higher than  $J_c$ . In our case the current in the belt is as high as  $J_e^0 + J_c$  at the beginning of the local flux penetration, e.g., higher than  $J_c$ . Moreover, as shown in Ref. [10], an ordered vortex crystal is able to continue to move coherently even under the action of driving forces much smaller than the recrystallization force. Thus, once a coherent region has appeared, it moves farther into the sample. As long as new vortices penetrate from the sample edge, the ordered region grows, forming a flux droplet of lower flux density than  $H_a$ . Growth continues probably until the current redistribution decreases the driving force on the droplet front below some pinning-determined value of the critical force  $F_p$ .

It is useful to point out that droplet formation has the same effect on the course of field penetration as the filling of the interior of the sample by vortices according to Zeldov’s model with  $J_c \lesssim J_e^0$ . Upon increasing the field to  $H_a > H_p$ , both mechanisms lead to a decrease of the sample region with nonzero screening currents, and it fulfills the new equilibrium condition  $J_y(W_{\text{eff}} - d/2) \leq J_e^0 + J_c$  on the edges.

Alternatively, droplet growth may be stopped due to the creation and accumulation of defects in the “perfect” vortex lattice. For a coherently moving vortex crystal the effect of the pinning potential is averaged out by the lattice periodicity. Any defect, like a dislocation, appearing in the moving lattice will suppress this averaging, and a pinning force develops that impedes the motion. The remark with respect to time scales can be made. Given the current the typical flux-flow velocity  $v = \rho_0 B / \mu_0 B_{c2} d$  is of order 1.0 m/s, leading to the time scale  $\tau \sim 100 \mu\text{s}$  of the droplet formation. Here  $\rho_0 \approx 6 \mu\Omega \text{ cm}$  is the normal state resistivity, and the Bardeen-Stephen expression for flux-flow resistivity has been used. Decoration itself takes a second, suggesting that the stopping process is intrinsic.

Another argument in favor of collective vortex motion is the observation that one of the close-packed directions of the vortex lattice inside the droplet, near the front, was always found to be perpendicular to the front curvature, e.g., along the direction of droplet motion (see Fig. 3).

This is consistent with earlier theoretical predictions [11] for the lattice orientation in a moving vortex crystal.

Once stopped, a perfect vortex crystal is expected to relax, being subject to both pinning potential and thermally induced disorder. While the spatial variations of the pinning potential are of the order of  $\xi$ , and its influence cannot be seen on the decoration patterns, thermally induced fluctuations can actually introduce a certain degree of disorder. But in contrast with field-cooling experiments, where the lattice forms from the disordered liquid state near  $T_c$ , droplets appear at low temperatures where  $c_{66}$ , the shear modulus of the vortex lattice, always has a nonzero value. It can lead to the preservation of the highly ordered state observed in the droplets. This is also suggested by the fact that in zero-field-cooling experiments, where the field was applied at 4.2 K, droplets are seen as well, but the order inside them has decreased. We found an orientational correlation length value of about  $10a_0$  in this case (compared to about  $300a_0$  in the experiments described above). This again suggests that droplets penetrate during field application and not during the heating in the decoration procedure.

Finally we performed experiments at an external field of 7.5 mT, which should be above the barrier field. In this case the field has filled the whole sample except for a vortex-free region, along the edges. The filling of the sample interior indicates that the condition  $J_c \lesssim J_e^0$  indeed holds, otherwise we would simply find a belt with increased width, according to [2]. The width of the vortex-free region was found to be smaller (10–15  $\mu\text{m}$ ) than predicted by Zeldov's model (40–60  $\mu\text{m}$  for typical sample sizes). The induction in the samples is approximately equal to the applied field, and we do not see any substantial field gradient from the boundary of the vortex-free region towards the sample center. In fact, the vortex distribution observed is more similar to the field-cooled case. It is important to emphasize that Zeldov's model deals with the penetration of individual vortices and does not consider any possible collective phenomena, like formation of the droplets we observed. Therefore we might expect the final field distribution to be different from the Zeldov's equilibrium state at  $H_a > H_p$ .

In conclusion, we performed direct observations of the geometrical barrier effect. We observed an unusual type of flux penetration via flux droplet formation. The vortex pattern inside the droplets has a much larger orientational correlation length than the field-cooled patterns of the correspondent fields. The geometrical barrier effect creates a unique situation in low pinning materials that leads to the appearance of the coherent flux-flow regime at the penetration field and to the formation of flux droplets.

We are indebted to J. V. Waszczak for the NbSe<sub>2</sub> single crystals and to G. Blatter and E. Zeldov for stimulating discussions. This work is part of the research program of the "Stichting voor Fundamenteel Onderzoek der Materie," which is financially supported by "NWO." L. A. G. acknowledges the financial support from NATO Linkage Grant No. 930049.

- 
- [1] E. H. Brandt, Phys. Rev. B **46**, 8628 (1992).
  - [2] E. H. Brandt and M. Indenbom, Phys. Rev. B **48**, 12 893 (1993).
  - [3] E. Zeldov, J. R. Clem, M. McElfresh, and M. Darvin, Phys. Rev. B **49**, 9802 (1994).
  - [4] E. Zeldov, A. I. Larkin, V. B. Geshkenbein, M. Konczykowski, D. Majer, B. Khaykovich, V. M. Vinokur, and H. Shtrikman, Phys. Rev. Lett. **73**, 1428 (1994).
  - [5] M. V. Indenbom, H. Kronmüller, T. W. Li, P. H. Kes, and A. A. Menovsky, Physica (Amsterdam) **222C**, 203 (1994).
  - [6] U. Essmann and H. Träuble, Phys. Lett. **24A**, 526 (1967).
  - [7] L. Ya. Vinnikov, I. V. Grigorieva, and L. A. Gurevich, in *The Real Structure of High  $T_c$  Superconductors*, edited by V. Sh. Shekhtman (Springer-Verlag, Berlin, Heidelberg, 1993), p. 89.
  - [8] W. DeSorbo and W. A. Healy, Cryogenics **4**, 257 (1964).
  - [9] A. Duarte, E. Fernandez Righi, C. A. Bolle, F. de la Cruz, P. L. Gammel, C. S. Oglesby, B. Batlogg, and D. J. Bishop (to be published).
  - [10] A. E. Koshelev and V. M. Vinokur, Phys. Rev. Lett. **73**, 3580 (1994).
  - [11] A. Schmid and W. Hauger, J. Low Temp. Phys. **11**, 667 (1973).

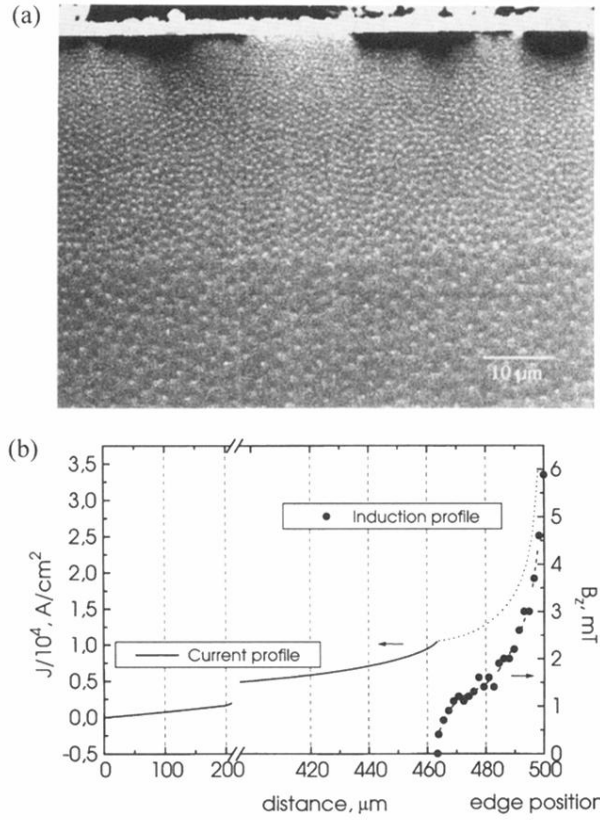


FIG. 1. (a) Decoration pattern of the vortex distribution in the belt near the sample edge,  $H_a = 3$  mT. (b) Induction profile in the sample as measured from the above picture and the corresponding current distribution, calculated (see text) for a sample half-width  $W = 0.5$  mm and thickness  $d = 130$   $\mu\text{m}$ . The value at the edge was not measured, but fixed at  $H_{\text{edge}} = H_a \sqrt{W/d} \approx 5.9$  mT. Close to the edge the current distribution (dotted) is most affected by the fixed value of  $H_{\text{edge}}$ .

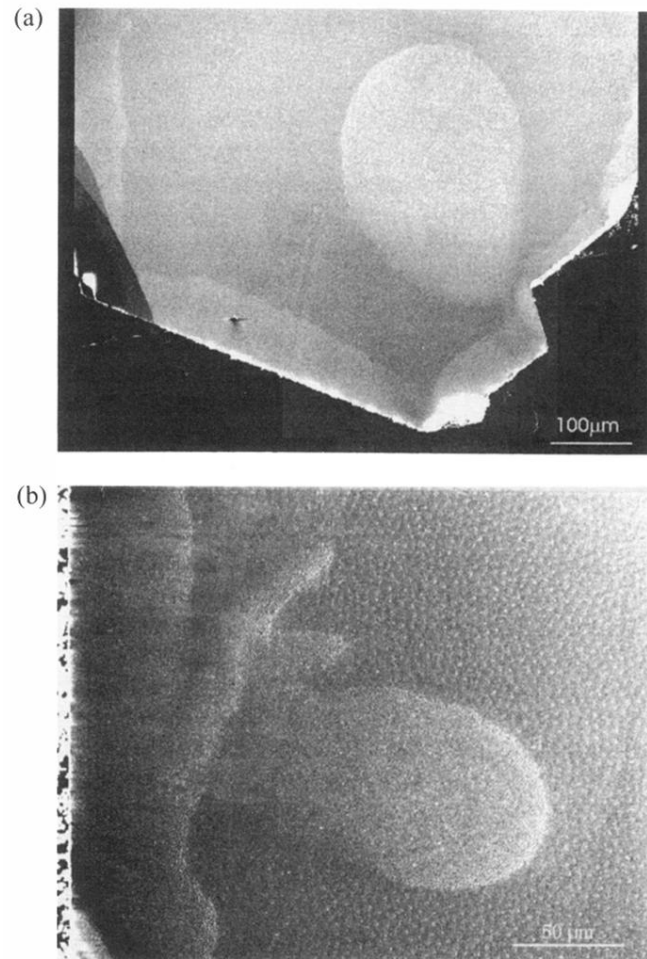


FIG. 2. Decoration patterns obtained on different samples at  $H_a = 5$  mT. Visible are parts of the sample edge, with the belt and droplets originating from it.

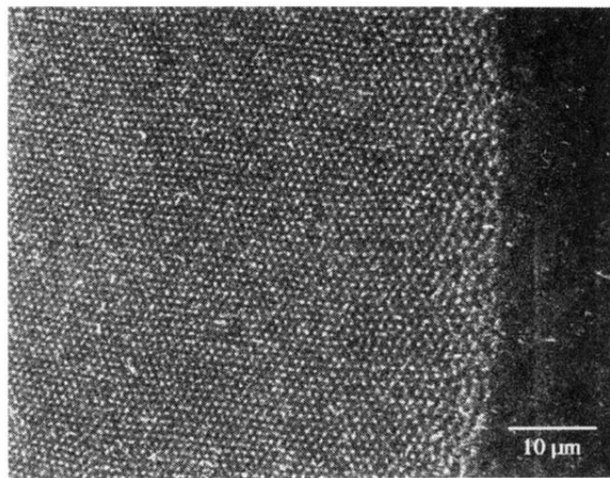


FIG. 3. A higher magnification view of the vortex pattern in the flux droplet close to its front (calculated induction 2.2 mT).